Influence of surface waves on measured and modeled irradiance profiles

J. Ronald V. Zaneveld, Emmanuel Boss, and Andrew Barnard

Classical radiative transfer programs are based on the plane-parallel assumption. We show that the Gershun equation is valid if the irradiance is averaged over a sufficiently large area. We show that the equation is invalid for horizontal areas of the order of tens of meters in which horizontal gradients of irradiance in the presence of waves are much larger than vertical gradients. We calculate the distribution of irradiance beneath modeled two-dimensional surface waves. We show that many of the features typically observed in irradiance profiles can be explained by use of such models. We derive a method for determination of the diffuse attenuation coefficient that is based on the upward integration of the irradiance field beneath waves, starting at a depth at which the irradiance profile is affected only weakly by waves.

OCIS codes: 010.4450, 030.5620, 000.4430, 070.4560.

1. Introduction

Optical remote sensing by use of satellites averages the upwelling radiance over the footprint of the satellite. For the Sea-Viewing Wide Field-of-View Sensor (SeaWiFS) this is approximately 1 km × 1 km. When the experimental optical oceanographer goes to sea to undertake observations to calibrate the satellite data or to validate inversion algorithms, he or she typically takes measurements from a ship using profiling radiometers and profiling devices for the measurement of absorption, scattering, and attenuation characteristics (inherent optical properties, IOP's). Observations from ships or moored profilers have a footprint of less than 1 m × 1 m. It is then usually assumed [for example, in NASA's Sensor Intercomparison and Merger for Biological and Interdisciplinary Oceanic Studies (SIMBIOS) program] that the shipboard observation is a valid ground truth measurement for the one million times larger satellite footprint. It is clear that the much larger satellite footprint averages over many more surface waves than an *in situ* profile. Because of this, shipboard irradiance profiles nearly always show large variations in the absolute value of the downwelling irradiance near the surface. Figures 1 and 2 show typical measured profiles. Variability in the irradiance is largest near the surface, yet for remote sensing purposes near-surface measurements are by far the most important.

Much has been written about the statistics of the light field variations caused by surface waves. The book by Walker[1] gives a thorough review on the subject, including extensive literature from Poland and the former Soviet Union. Near-surface fluctuations in measured irradiance profiles are usually treated as noise and are filtered out.[2] In this paper we show that the horizontal gradient in irradiance profiles is often an order-of-magnitude larger than the vertical gradient. An individual irradiance profile clearly shows the superposition of wave-induced irradiance fluctuations on the vertical profile. Here we address the vertical structure of irradiance profiles in the presence of waves and examine the variability of these profiles for constant light absorption and scattering conditions (IOP's) and its influence on radiative transfer. We examine characteristic vertical structures of these profiles and relate them to sea surface properties.

2. Plane-Parallel Assumption

When radiometric data are used to infer IOP's, or when radiative transfer calculations are performed, it is often assumed that the ocean is horizontally

J. R. V. Zaneveld (zaneveld@oce.orst.edu), E. Boss (eboss@oce.orst.edu), and A. Barnard (abarnard@oce.orst.edu) are with the College of Oceanic and Atmospheric Sciences, Oregon State University, 104 Ocean Administration Building, Corvallis, Oregon 97331-0000.

Received 7 July 2000; revised manuscript received 6 November 2000.

0003-6935/01/091442-08$15.00/0

homogeneous. This is the so-called plane-parallel assumption. This assumption has major implications for the understanding and applicability of shipboard data to radiative transfer modeling.

If the equation of radiative transfer is integrated over 4π sr, we derive Gershun's[3] equation:

$$\nabla \cdot E(x, y, z) = -a(x, y, z)E_0(x, y, z), \tag{1}$$

where E is the net plane irradiance, a is the absorption coefficient, and E_0 is the scalar irradiance. This equation is almost always cited in the oceanographic literature as

$$\frac{\mathrm{d}E(z)}{\mathrm{d}z} = -a(z)E_0(z), \tag{2a}$$

or

$$K(z)E(z) = a(z)E_0(z), \tag{2b}$$

or

$$\frac{a(z)}{K(z)} = \frac{E(z)}{E_0(z)} = \bar{\mu}(z), \tag{2c}$$

where $K(z)$ is the attenuation coefficient for the plane irradiance and $\bar{\mu}(z)$ is the average cosine of the light field. These equations (which we refer to as the plane-parallel Gershun or PPG equations) imply that the horizontal gradients in E are small compared with the vertical ones. Thus the plane-parallel assumption implies that

$$\frac{\partial}{\partial x}E(x, y, z) \ll \frac{\partial}{\partial z}E(x, y, z),$$

$$\frac{\partial}{\partial y}E(x, y, z) \ll \frac{\partial}{\partial z}E(x, y, z). \tag{3}$$

We examine whether the large-scale horizontally averaged irradiance profile obeys the PPG equations.

3. Near-Surface Horizontal and Vertical Gradients of Irradiance

The sea surface nearly always contains at least some small waves. Typical downwelling plane irradiance profiles for off the Oregon coast and the Gulf of California are shown in Figs. 1 and 2. These profiles were taken under calm conditions (winds were less than 2 m/s for Fig. 1 and less than 0.5 m/s for Fig. 2). Near the surface the profiles fluctuate by a factor of 2–3 several times at a depth interval of 1 m. These fluctuations are not due to small-scale vertical variations in the IOP's because the IOP measurements that were made almost simultaneously show uniform vertical profiles. A tilt sensor in the instrument showed values of approximately 1 deg for these profiles. The irradiance fluctuations are thus almost entirely due to variations in the underwater light field related to the wavy surface.

We now calculate approximately the horizontal and vertical gradients of the irradiance for the profile in Fig. 2, taken during quite calm conditions in the

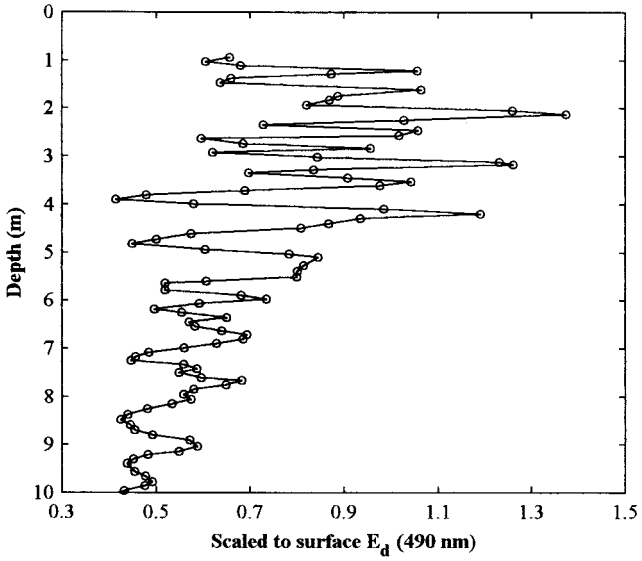

Fig. 1. Irradiance profile taken off the Oregon coast, September 1997, with a Satlantic irradiance profiler. The profiler drops at approximately 0.8 m/s and samples at 8 Hz. Conditions were calm.

Gulf of California. The profiler with which the data were obtained drops at approximately 80 cm/s, and the vertical peaks of irradiance in Fig. 2 (in the Gulf of California) were measured approximately 0.4 s apart. If we assume that these peaks are due to a wave with a period T of approximately 0.4 s, we find that for gravity waves in deep water[4] their wavelength is approximately 0.7 m (using $T^2 = 1/gk$, where g is the gravitational constant and k is the wave number). If we assume that E is proportional to $\sin(kx)$, we can see that $(\partial/\partial x)E(x, z)$ is proportional to $k\cos(kx)$ and the average value of the horizontal gradient of E, $< (\partial/\partial x)E(x, z) > \approx (k/2)E \approx$

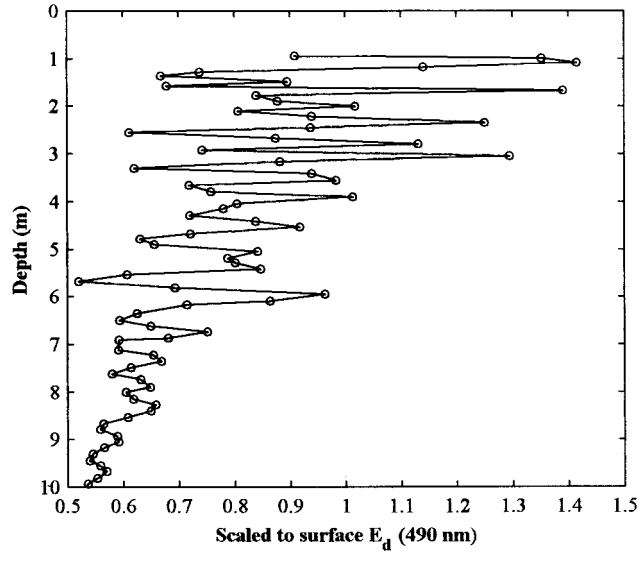

Fig. 2. Irradiance profile taken in the Gulf of California, October 1998, with the same profiler as used in Fig. 1. Conditions were calm.

4.5 E. On the other hand, the total absorption coefficient was measured to be 0.1 m^{-1}. With $\bar{\mu} \approx 0.8$ and using Eqs. 2(a)–2(c), we see that $(\partial/\partial z)E(x, z) \approx 0.1/0.8 = 0.125\,E$. The horizontal gradient near the surface is thus more than an order-of-magnitude larger than the vertical gradient. The conditions in inequalities (3) therefore do not apply at all, and the ocean is anything but horizontally homogeneous as far as irradiance is concerned. It should be noted that the example just provided is for extremely calm oceanic conditions. For conditions with larger waves, the horizontal gradients would be larger. For the PPG equations to apply, the horizontal gradient of irradiance would have to be approximately 2 orders-of-magnitude smaller than that observed in the ocean under calm conditions.

4. Large-Area Approximation of the Gershun Equation

Given that the plane-parallel assumption does not apply to typical ocean surfaces over a horizontal scale of meters, even if the IOP's are constant, does it apply for kilometer scales? We show here that it does indeed apply when irradiances are averaged over suitably large areas, and the PPG equation [Eq. (2)] can be used for irradiances averaged horizontally over large scales.

For simplicity we use the two-dimensional form of Eq. (1):

$$\frac{\partial}{\partial x}E(x, z) + \frac{\partial}{\partial z}E(x, z) = -a(z)E_0(x, z), \qquad (4)$$

where the absorption coefficient is assumed to be a function of z only.

Integrating Eq. (4) from x_1 to x_2, we obtain

$$E(x_1, z) - E(x_2, z) + \int_{x_1}^{x_2} \frac{\partial}{\partial z}E(x, z)\mathrm{d}x = -a(z)\int_{x_1}^{x_2} E_0(x, z)\mathrm{d}x. \qquad (5)$$

We then divide by Δx and denote the average over x by an overbar:

$$\frac{E(x_1, z) - E(x_2, z)}{\Delta x} + \frac{\partial}{\partial z}\overline{E(z)} = -a(z)\overline{E_0(z)}. \qquad (6)$$

In the limit of $\Delta x \to \infty$, we obtain

$$\frac{\partial}{\partial z}\overline{E(z)} = -a(z)\overline{E_0(z)}. \qquad (7)$$

We have thus shown that large horizontal averages of plane and vector irradiance obey the plane-parallel approximation and the PPG equation. How large a horizontal area needs to be averaged in practice? In the above example we had variations approximately of the magnitude of E in one wavelength of approximately 0.7 m which gave a gradient of 4.5 E. The vertical gradient was estimated to be an order-of-magnitude smaller. To invert this, with the horizontal component being an order-of-magnitude smaller than the vertical gradient, we would have to average over 100 wavelengths, or approximately 70 m in this case for calm conditions. In the presence of a large swell with wavelengths of tens of meters, 100 wavelengths could well exceed the footprint of the satellite radiance sensor. Note that the above does not imply that the large-scale average irradiance is the same in the presence of waves as in their absence.

5. Model for Radiometer Profiles under Waves

When the experimentalist measures the profile of a radiometric property in a wavy environment, a single realization of the profile is obtained. Such profiles depend on the specific location at which the profile is taken. Averages of several different profiles will differ, yet it is usually assumed that such averages represent the large-scale average. For that to be true, the ergodic principle must hold, and a sufficiently large number of profiles must be averaged to satisfy the conditions in inequalities (3). In Section 6 we study the relationship of a single realization of the irradiance profile to the large-scale average. So far we have dealt with the net plane irradiance $E(z)$. The parameter that is usually measured is the downwelling plane irradiance $E_d(z)$. In practice these two quantities differ by only a few percent. For practical purposes, the scale arguments made for the net plane irradiance thus also apply to the downwelling irradiance. We are particularly interested in determining how such single profiles can be depth or space averaged to obtain an approximation of the large-scale average $\overline{E_d(z)}$. It is obvious from the above discussion that averaging a large number of profiles of $E_d(z)$ will approximate the large-area average $\overline{E_d(z)}$.

Many radiative transfer models take waves into account. In such models[1,5] the radiance just beneath the sea surface is nevertheless assumed to be horizontally homogeneous. We can accomplish this by using the statistics of the wave slopes and by obtaining an ensemble-average radiance distribution. This radiance distribution would be the same as the large-area average alluded to above provided that all the waves are taken into account (we show below that even small waves have a significant impact on the underwater light field). Such radiative transfer models thus apply to remote sensing problems when the conditions in inequalities (3) are met. They do not apply when we want to understand in more detail the experimental vertical irradiance profiles such as those in Figs. 1 and 2.

To study the effects of waves on vertical irradiance profiles, we developed a two-dimensional wave model that allows us to model measured radiometer profiles under a variety of wave conditions. Our model takes parallel incident rays, refracts them at the sea surface according to Snell's law, and reduces their intensity according to the Fresnel equations. The locations of intersection with the z plane and angle of incidence are calculated. By using a large number

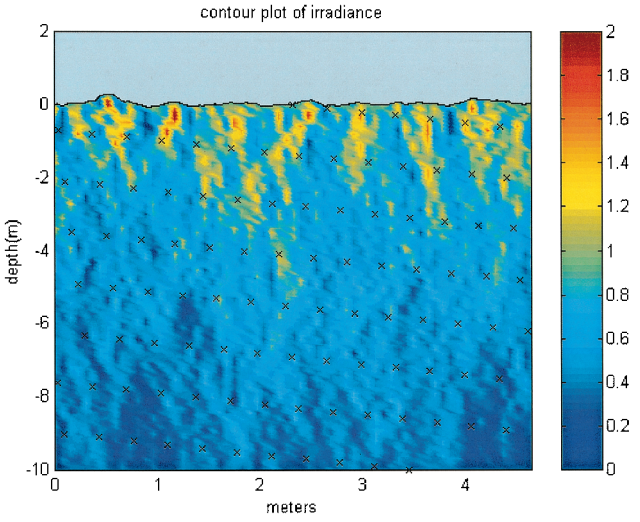

Fig. 3. Irradiance pattern beneath a random wave surface with a 1.1-m dominant wave: $a = 0.06\ \mathrm{m}^{-1}$ and $b = 0.15\ \mathrm{m}^{-1}$. A Petzold volume-scattering function was used (see text). Crosses are sampling points of an irradiance sensor dropping at 0.8 m/s with a sampling rate of 8 Hz.

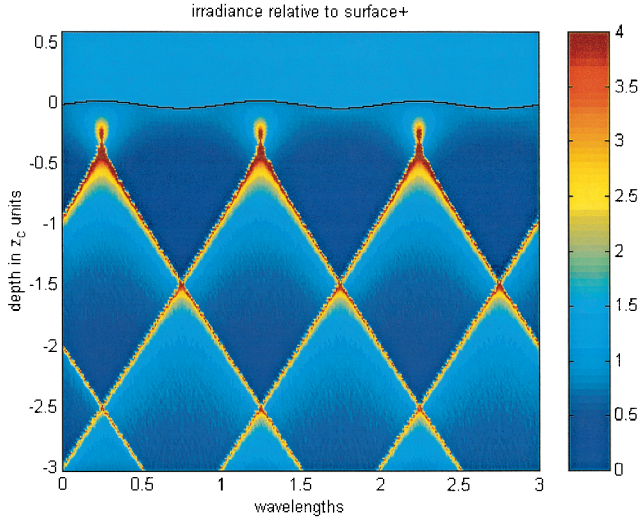

Fig. 4. Irradiance pattern beneath a generic sine wave. The vertical extent of the basic diamond pattern is a function of the wavelength and wave steepness only (see text).

of rays and by sorting their irradiances according to the intersection with the z plane, we can obtain the irradiance as a function of distance along the z plane. We add absorption and scattering effects by turning each ray intersection with z into a beam spread function pattern and recalculating the distribution of E along z. To do this we follow the model of McLean and Freeman,[6] which in turn is based on the theoretical development of Wells.[7] The program that we developed allows the superposition of any number of sinusoids and use of any spatial distribution of the absorption coefficient and volume-scattering function. Solar zenith angle and sky conditions will affect the results. In this paper we chose to limit the already extensive number of parameters that affect the underwater irradiance distribution. We therefore used a vertical Sun in a black sky and homogeneous IOP's. Figure 3 is an example of the output of our radiative transfer program. In this example we calculated the downwelling irradiance pattern relative to the downwelling irradiance just above the surface for homogeneous IOP's and a random wave surface with a 1.1-m dominant wave. Figure 3 also shows the sampling points of a typical irradiance profiler, which is discussed further below.

The ray pattern beneath a sinusoidal wave has been studied before[1]; we present additional details here. We calculated the irradiance fields beneath wave surfaces of increasing complexity to study their influence on the spatial distribution of downwelling irradiance. Figure 4 shows the plane irradiance beneath a one-dimensional sinusoidal wave. No absorption or scattering of light was introduced. An obvious feature is the extreme horizontal variation of $E_d(z)$, with a focal area beneath the wave crest. Note that the focal point is spread out because we do not have a simple spherical surface. Also note that beams from successive waves intersect multiple times below the primary focal area and form a diamond pattern. These beams are due to the sinusoidal wave form, which has two nearly flat areas at $z = 0$. These areas generate nearly parallel rays unlike the converging or diverging rays from the rest of the sinusoidal surface. These beams persist to great depths if not diffused by scattering. When there is weak absorption and scattering, the maximum irradiance occurs in the primary focal point and the minimum just above the first intersection of the beams from successive waves. These minima decrease in intensity with depth because, at each successive crossover, the light from more waves is averaged. Simple geometry shows that the vertical size of the diamond pattern is given by

$$z_c = \frac{L}{2}\tan\left(\frac{\pi}{2} + a\,\sin\left\{\frac{1}{n}\sin\left[a\,\tan\left(\frac{2\pi A}{L}\right)\right]\right\} - a\,\tan\left(\frac{2\pi A}{L}\right)\right), \tag{8}$$

where n is the index of refraction of the water, A is the amplitude, and L is the wavelength of the sinusoidal wave. A/L is the wave steepness.

Various authors[1] have approximated the depth of the focal area. Our own calculation is based on the assumption that the crest of the wave can be approximated by a spherical segment with the same amplitude-to-wavelength ratio (A/L) as the wave. This approximation gives the depth of the focal point as

$$\frac{z_f}{L} = 2\frac{A}{L} + \frac{1}{8}\frac{L}{A}, \tag{9}$$

where z_f is the depth of the focal point below the average surface elevation. The ratio of the focal

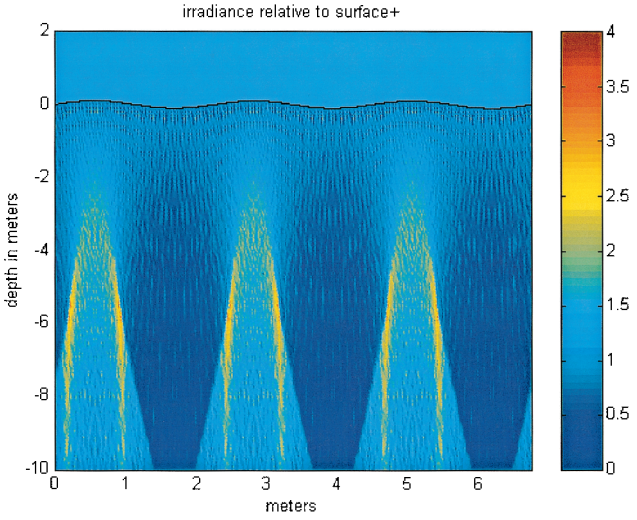

Fig. 5. Downwelling irradiance field beneath a sea surface composed of a gravity and a capillary wave. The gravity wave has a wavelength of 2.25 m and an amplitude of 0.1 m. The capillary wave has a wavelength of 0.05 m and an amplitude of 0.002 m.

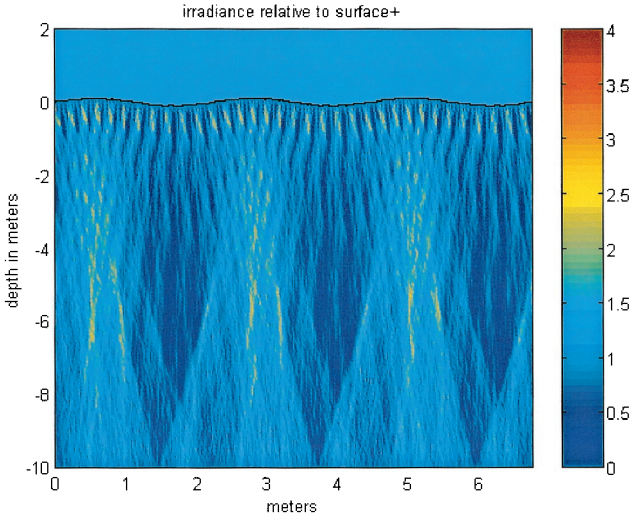

Fig. 6. Irradiance pattern beneath a superposition of sinusoidal waves with wavelengths of 2.25, 0.2, and 0.05 m and with amplitudes of 0.1, 0.01, and 0.002 m. Note that the addition of very small amplitude waves significantly alters the irradiance pattern.

depth to the wavelength, z_f/L, depends only on the wave steepness.

The irradiance pattern beneath a sinusoidal wave can thus be scaled in the x direction to wavelength L and in the z direction to the fundamental size of the diamond pattern described above. With this scaling in mind, Fig. 4 thus applies to the light pattern beneath any sinusoidal wave. Note that absorption and scattering were neglected here to show a clear picture of the irradiance pattern.

Figure 5 shows a wave with $L = 2.25$ m and $A = 0.1$ m with the addition of a capillary wave with a wavelength of 0.05 m and an amplitude of 0.002 m. It can be immediately seen that such a very small capillary wave completely changes the underwater irradiance pattern from that of a simple sinusoid. The focal beams of the 1-m wave alluded to above are greatly reduced in intensity. Figure 6 shows the addition of a smaller wave with a wavelength of 0.2 m and a 0.01-m amplitude to the wave in Fig. 5. The change also emphasizes that very small ripples in the sea surface have a significant effect on the underwater irradiance distribution. It can be seen that the number of focal areas are increased by the number of wave crests added and that their divergence below and above the focal area is governed by the wavelength and the wave steepness. When diving or looking over the side of a ship, one can see that these narrow, well-defined rays converge. The apparent convergence is due to the perspective of parallel rays that meet at infinity.

The strong dependence of the near-surface irradiance distribution on the surface waves has a major influence on the measured vertical profile of irradiance. To model the dependence of the measured vertical irradiance profile on the surface waves, we carry out the following analysis. The radiometer profiler drops through the water at a speed w_d. The largest wave travels horizontally at a wave speed v_w. Thus we can visualize the track of the profiler through the irradiance field beneath the waves by considering the waves to be stationary and the instrument to be descending at a speed of w_d while traveling horizontally at a speed v_w. This approach is not exactly correct inasmuch as the different waves that constitute the surface travel at different speeds (wave dispersion). The method works well enough, however, to understand observed $E_d(z)$ profiles. Figure 3 shows the track of a profiler through a random wave surface generated by the superposition of a number of sinusoids. This wave surface corresponds to a wind speed of 10 m/s.

The ensemble of possible profiles has some interesting characteristics. Figure 7 shows the superposition of 20 irradiance profiles with random starting points in the surface wave pattern. Irradiance profiles were calculated for a profiler with a drop speed of 0.8 m/s and a sampling rate of 8 Hz. The greatest variance occurs between 2 and 3 m, the focal area of the largest wave. The variance decreases below the focal area and decreases sharply at 6 m. This is the depth of the intersection of the focal rays discussed above. Beneath this point the light from more waves is averaged, reducing the variance. It can also be seen that the minimum irradiance at a given depth actually increases below 6 m for the same reason.

6. Analysis and Reconstruction of Irradiance Profiles

Using the above model results we are now in a position to understand features of specific profiles much better. Figure 2, for example, shows a region of maximum variance between 2 and 5 m, which is presumably the focal area of the largest wave. The

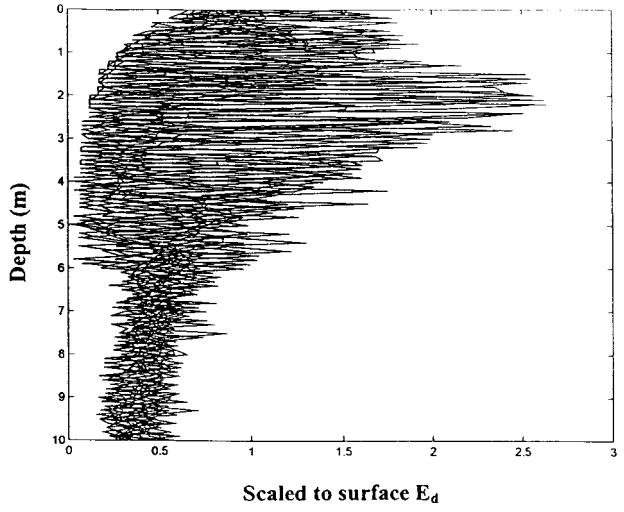

Fig. 7. Superposition of 20 modeled irradiance profiles with random offsets. $a = 0.1\ m^{-1}$ and $b = 0\ m^{-1}$. The surface consists of two waves with wavelengths of 2.25 and 0.2 m and amplitudes of 0.29 and 0.01 cm, respectively.

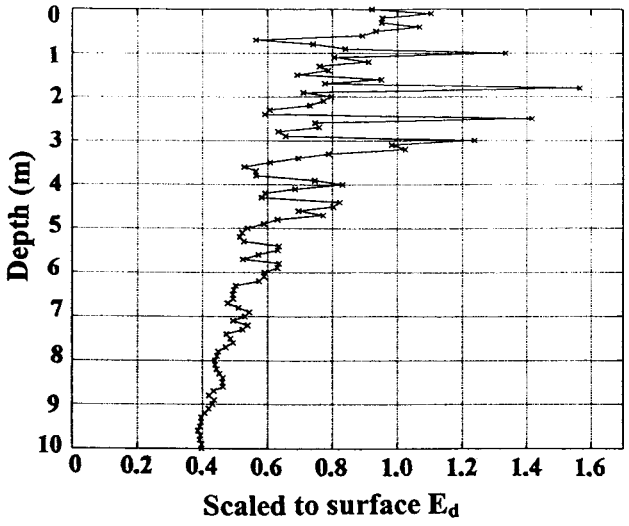

Fig. 8. Modeled irradiance profile with waves of wavelengths 3, 1.2, 0.6, and 0.05 m and amplitudes of 0.1, 0.05, 0.01, and 0.0006 m, respectively. $a = 0.07\ m^{-1}$, $b = 0.39\ m^{-1}$, offset is 0.355 m, and drop speed is 0.6 m/s.

minimum irradiance in the 10-m profile occurs just above a 6-m depth, not at the greatest depth. Below 6 m the profile is much more damped, indicating that 6 m is probably the depth of the crossover point of the focal rays. Finally, the profile is increasingly smooth, probably because of light scattering, although the presence of capillary waves would also contribute to damping of irradiance fluctuations.

We have already shown that the irradiance pattern beneath a wave is highly dependent on even the smallest surface elevations and the specific location in the wave train where the profile is taken. The reconstruction of a specific measured wave profile thus is not possible. One can, however, generate profiles that display similar features to the measured one by varying the components of the surface wave, the starting location in the wave train, and the drop speed. For the profile in Fig. 2, for example, we measured the IOP's to be absorption coefficient $a = 0.07\ m^{-1}$ and scattering coefficient $b = 0.39\ m^{-1}$. We can estimate the period of the dominant wave from the measured profile by determining the time interval of vertical irradiance maxima in the profile. The wavelength is then calculated from the period. Figure 8 shows an irradiance profile generated by use of the measured IOP's and an average Petzold phase function.[5] The modeled profiles are extremely sensitive to the details of the surface, the point in the wave pattern at which the probe enters the water, and the drop speed of the probe.

7. Determination of an Average Diffuse Attenuation Coefficient

The attenuation coefficient of the downwelling plane irradiance $K_d(z)(\equiv -1/E_d \partial E_d/\partial z)$ is a frequently used parameter in remote sensing algorithms. Its determination from a single profile of irradiance beneath a wavy surface is not straightforward. Depending on where in the wave train the profiler penetrated the surface, one obtains a different profile. These profiles will provide larger or smaller K_d values near the surface depending on whether they profiled through a focal region. It is not unusual to see an irradiance profile with the maximum at a 2–3-m depth. This does not imply that the maximum large-scale horizontally averaged irradiance occurs at that depth, but only that the local irradiance measured during the profile had a maximum. Such local profiles in turn can lead to a negative K_d value in the upper 2–3 m if any of the usual averaging schemes are used. Similarly, analysis of single profiles can lead to K_d values that are less than the absorption coefficient. One method is to take many profiles and to average them. In the limit, this approaches the horizontal average irradiance at each depth.

It was shown that the PPG equation holds for the horizontally averaged light field. Let the horizontally averaged downwelling irradiance be given by $\overline{E_d(z)}$. We measure a single realization of $E_d(z)$ beneath a wavy surface. Each profile is different even though $\overline{E_d(z)}$ remains constant. Is there an optimum way to derive K_d for $\overline{E_d(z)}$ when we have only a single profile of $E_d(z)$?

We assume that $\overline{E_d(z)}$ has an exponential profile $\overline{E_d(z)} = \overline{E_d(0)}\exp(-K_d z)$. If we wish to obtain an estimate of the depth-integrated irradiance present between a depth z_0 at which fluctuations in irradiance that are due to the sea surface are small and the sea surface, we could write

$$I = \int_{z_0}^{0} \overline{E_d(z)}\,dz = \frac{\overline{E_d(0)}}{K_d}[\exp(K_d z_0) - 1]. \quad (10)$$

We obtained the integrated irradiance I, in numerical practice, by subdividing space into small volumes $\Delta x \Delta z$ and allowing $E_d(x, z)$ to represent the value of the irradiance in the immediate neighborhood. Integration by use of the sampling points of the irradiance profiler uses the same principle, but the sampling points (x, z) are different. We thus can set integration over the two sets of sampling points approximately equal; in the limit of infinitely close spacing of Δx and Δz, they would be

$$I' = \int_{z_0}^{0} E_d(z)\mathrm{d}z \approx \frac{\overline{E_d(0)}}{K_d}\,[\exp(K_d z_0) - 1]. \quad (11)$$

This would be sufficient to determine K_d if we knew $\overline{E_d(0)}$, but, given single irradiance profiles, this is difficult to determine. We can avoid having to know $\overline{E_d(0)}$ by integrating from z_0 to successively shallower z:

$$I'(z) = \int_{z_0}^{z} E_d(z)\mathrm{d}z \approx I(z) = \frac{\overline{E_d(0)}}{K_d}\,[\exp(K_d z_0) - \exp(K_d z)]. \quad (12)$$

We then see that the slope of $\ln[\mathrm{d}I'(z)/\mathrm{d}z]$ is K_d.

For profiles such as those shown in Figs. 1 and 2, one can choose $z_0 = 10$ m, integrate the profile from 10 to 9 m, from 10 to 8 m, etc. to obtain $I'(9), I'(8)$, etc. K_d is calculated when we least-squares fit an exponential to $\Delta I'(z)/\Delta z$.

We ran an example of a superposition of three sinusoidal waves. The absorption coefficient was set at 0.05 m^{-1}. The scattering coefficient was set at 0 m^{-1} so that K_d was highly predictable. In the absence of scattering, only the increased path length that was due to the refraction at the sea surface causes K_d to deviate from a. This deviation is, however, small. We thus know that the large-scale K_d is nearly equal to 0.05 m^{-1}. How do K_d's for individual profiles deviate from the large-scale K_d? The statistics for 2000 calculated profiles through the wave-induced irradiance field were as follows: mean K_d = 0.0503 m^{-1}, median K_d = 0.0503 m^{-1}, standard deviation of 0.0037 m^{-1}, $K_{\min}$ = 0.0413 m^{-1}, and $K_{\max}$ = 0.0597 m^{-1}. The distribution of K_d values was nearly Gaussian. Thus the mean K_d was very close to a as expected. K_d's for individual profiles showed deviations as large as 20%. Thus it is perfectly reasonable for the K_d determined from an individual profile to be less than the absorption coefficient because not all the divergence in $E_d(x, z)$ is contained in the vertical direction.

8. Discussion and Conclusions

We have shown that the variability of irradiance profiles as typically determined by experimentalists is not due to instrument noise, but probably represents the true irradiance field as present beneath the wavy sea surface. Even waves with small amplitudes have a significant effect on the redistribution of irradiance [Figs. 4 and 5; Eqs. (8) and (9)]. Current commercially available irradiance sensors typically drop at 0.8 m/s and sample at 8 Hz. Because of the statistical nature of the sea surface and the discrete sampling of the irradiance field, it is to be expected that no two irradiance profiles will be the same, even though the wind speed and IOP's are constant. This observation is supported by Fig. 7 in which 20 irradiance profiles are superimposed. For these same 20 profiles, the IOP profiles are identical. Whereas one measured IOP profile when used with appropriate wave statistics can lead to the calculation of an accurate, spatially averaged irradiance profile (by use of the plane-parallel assumption and classical radiative transfer), one measured irradiance profile (or a combination of other local radiometric measurables) cannot be inverted to obtain the IOP accurately, even if the wave statistics are known. Simply stated, waves directly affect apparent optical properties, but not IOP's. Indirectly, of course, breaking waves generate bubbles that in turn affect the IOP's.

Zaneveld[8] showed that IOP's can be uniquely determined if the radiance and its depth derivative are known. We have shown here that this proof applies only if the plane-parallel assumption is valid, i.e., if the horizontal gradient of the radiance is negligible.

We have shown that, for a sufficiently large horizontal scale, the horizontally averaged irradiance obeys the PPG equations [Eqs. (2a)–(2c)]. On that scale classical radiative transfer calculations based on the plane-parallel assumption can be used. For increasingly smaller scales, calculations based on these assumptions will show increasingly larger deviations between the model and the observations. We will direct our future research to comparing radiative transfer results using the plane-parallel assumption and wave optics models. This is of particular interest when we look at the remote sensing reflectance for different scales. Horizontal variability in the remote sensing reflectance is of particular interest as sensors are being developed with footprints of the order of tens of meters.

An important problem is the connection between a single irradiance profile and the large-scale average irradiance profile. It is obvious that within the limit of an infinitely high sampling rate and infinitely slow drop rates the two will converge. Irradiance profiles, however, are designed to drop quite fast to maintain vertical stability. We demonstrated that for such devices a value for the diffuse attenuation coefficient K_d can be derived [Eqs. (10)–(12)] that in the mean converges to the true large-scale K_d. Any individual calculation can still be in error, however. The standard deviation of the error depends on the wave surface as well as the IOP, so that no generalization can be provided. In the example provided, the standard deviation of the error was approximately 7%. This is fairly typical for wavelengths of the order of a meter.

The measurement of K_d by hanging irradiance sensors at a given depth below a mooring may have some

interesting consequences inasmuch as the sensors would follow the surface elevations and not be present at a constant depth relative to the average surface. This would result in an overestimate of the irradiance because of the averaging of an exponential function. The error would thus depend on the value of K_d.

In the calculations for Figs. 4, 5, and 6, we set the IOP equal to zero. We did this to show the results of wave focusing only. With increasing absorption, the irradiance values decrease with depth, whereas increased scattering smears the pattern. Stramska and Dickey[9] showed that the power spectrum of irradiance fluctuations in the green had a peak at a higher frequency than the wave power spectrum. The observation depths in their paper were 15 and 35 m. The focal depth for large L is approximately $1/8\ L^2/A$ [Eq. (9)]. The large waves thus will have focal depths beneath the observation point. The peak frequency of the irradiance fluctuation spectrum at a given depth will be due to the wave with a similar focal depth. In addition, IOP's will decrease the variance of irradiance with depth.

There are many expressions for the remote sensing reflectance as a function of the IOP. These also assume a plane-parallel situation because the upwelling radiance is less variable horizontally than the irradiance. Upwelling radiance taken at the same time as the irradiance, as shown in Figs. 1 and 2, has approximately 10% variability near the surface compared with the downwelling irradiance. The remote sensing reflectance ($R_{\mathrm{rs}} = L_u/E_d$) thus varies approximately inversely proportional to $E_d(z)$ with depth. Clearly this is not allowed under the plane-parallel assumption if the IOP's are constant with depth. The usual model,

$$R_{\mathrm{rs}} = \frac{f}{Q}\frac{b_b}{a}, \tag{13}$$

does not apply in a wavy environment on the scale of the wavelength of the surface wave. In the above example, where E varies by a factor of 2 at a wavelength of 70 cm, R_{rs} would also vary by approximately a factor of 2 horizontally at 70 cm, even though b_b and a are constants. The extension of this argument to wavelengths of tens of meters has implications for the interpretation of upwelling radiance signals taken with satellite sensors that have footprints of that order. Variability in the measured reflectance can be reduced when the downwelling irradiance is measured above the sea surface.

This research was supported by the Oceanography Program of the National Aeronautics and Space Administration.

References

1. R. E. Walker, *Marine Light Field Statistics* (Wiley, New York, 1994).
2. J. L. Mueller and R. W. Austin, "Ocean optics protocols for SeaWiFS validation, revision 1," NASA Tech. Memo. 104566, Vol. 25 S. B. Hooker, E. R. Firestone, J. G. Acker, eds. (NASA Goddard Space Flight Center, Greenbelt, Md., 1995).
3. A. Gershun, "On the theory of the light field in a scattering medium," C. R. (Dok.) Acad. Sci. URSS **49,** 556–557 (1945).
4. J. Lighthill, *Waves in Fluid* (Cambridge U. Press, Cambridge, UK, 1978).
5. C. D. Mobley, *Light and Water: Radiative Transfer in Natural Waters* (Academic, San Diego, Calif., 1994).
6. J. W. McLean and J. D. Freeman, "Effects of ocean waves on airborne lidar imaging," Appl. Opt. **35,** 3261–3269 (1996).
7. W. H. Wells, "Theory of small angle scattering," in *Optics of the Sea*, AGARD Lecture Series No. 61 (Advisory Group for Aerospace Research and Development, Neuilly-Sur-Seine, France, 1973), Sect. 3-3.
8. J. R. V. Zaneveld, "New developments of the theory of radiative transfer in the oceans," in *Optical Aspects of Oceanography*, N. G. Jerlov and E. Nielsen, eds. (Academic, London, 1974), pp. 121–134.
9. M. Stramska and T. D. Dickey, "Short-term variability of the underwater light field in the oligotrophic ocean in response to surface waves and clouds," Deep-Sea Res. I **45,** 1393–1410 (1998).